Titration Force Microscopy on Supported Lipid Bilayers

ARTICLE *in* ANALYTICAL CHEMISTRY · FEBRUARY 2006

Impact Factor: 5.64 · DOI: 10.1021/ac0510437 · Source: PubMed

3 AUTHORS, INCLUDING:

Pau Gorostiza
IBEC Institute for Bioengineering of Catalonia
112 PUBLICATIONS **2,710** CITATIONS
SEE PROFILE

Fausto Sanz
University of Barcelona
190 PUBLICATIONS **2,956** CITATIONS
SEE PROFILE

Anal. Chem. **2006,** *78,* 61−70

Titration Force Microscopy on Supported Lipid Bilayers

Sergi Garcia-Manyes,† Pau Gorostiza,‡ and Fausto Sanz*,†

Department of Physical Chemistry, Universitat de Barcelona, Martí i Franquès 1, 08028 Barcelona, Spain, and Department Molecular and Cell Biology, University of California at Berkeley, Berkeley, California 94720

The use of chemically modified atomic force microscopy (AFM) probes allows us to measure the surface charges of supported planar lipid bilayers with high sensitivity through the force spectroscopy operation mode. By controlling the chemistry of the tip, we can perform a classical analytical chemistry titration where the titration agent is a weak acid (attached to the AFM tip) with the particularity of being performed in surface rather than in solution and, especially, at the nanometric scale. Thus, the AFM tip acts as a real "nanosensor". The approaching curves of the force plots reveal that electrostatic interactions between the tip and the supported membrane play a key role. Besides, the plot of the adhesion force (measured from the retracting curve of the force plots) versus pH displays a nonsigmoidal shape with a peak in the adhesion force attributed to high-energy hydrogen bonds. One of these peaks corresponds to the pK_a of the surface under study and the other to the pK_a of the titrating probe attached to the tip.

In recent years, atomic force microscopy (AFM) has become a standard tool when it comes to imaging and studying the topography of all types of surfaces from a nanometric point of view.[1] Moreover, force spectroscopy mode has made it possible to measure the (nano-)mechanical properties of the surfaces and the interaction forces that arise between the surface and the measuring probe.[2] Indeed, the intermolecular forces near the surfaces in the nanometer scale play a key role in a wide range of chemical, biological, and physical processes, such as chemical and physical absorption, wetting, wear, catalysis, adhesion, cell recognition, etc. The involved interactions, especially when measured in a liquid environment, can be mainly explained in terms of van der Waals forces, electrostatic Coulombic interactions,[3] solvation forces, and hydrogen bonding.[4] Likewise, this technique has allowed one to study intrinsic properties of the matter of many different fields such as the deformation of materials at the nanometric scale,[5−8] the solvation forces arising between hydrophilic surfaces,[9] or the unfolding of single proteins[10] with piconewton resolution.

Interaction forces arising between a silica sphere or silica-coated sphere mounted on an AFM cantilever and the target substrate as a function of ionic strength and pH have been extensively used to examine the physicochemical properties of a wide number of substrates such as gold,[11,12] titania,[13] polystyrene latex,[14] sodium dodecyl sulfate,[15] octadecyltrimethylammonium chloride,[16] alumina,[17] polyelectrolytes,[18,19] cationic surfactants, or self-assembled monolayers.[20,21] From these studies, valuable information about the electrostatic properties of the surfaces together with their surface pK_a determination has been obtained. The use of thiol chemistry and the strong covalent S−Au bonding allows formation of self-assembled monolayers with different functionalities on gold-coated cantilevers. In general, the immobilized molecules are low molecular weight compounds, which in most cases contain only one functional group so that the interpretation of the results is facilitated.[22,23] Thus, the interaction forces between chemically derivatized surface and tip can be

* To whom correspondence should be addressed: E-mail: fsanz@ub.edu. Tel. +34 934021240. Fax: +34 934021231.

† Universitat de Barcelona.

‡ University of California at Berkeley.

(1) Binnig, G.; Quate, C. F.; Gerber, C. *Phys. Rev. Lett.* **1986**, *56*, 930−33.
(2) Capella, B.; Baschieri, P.; Frediani, C.; Miccoli, P.; Ascoli, C. *IEEE Eng. Med. Biol. Mag.* **1997**, *16*, 58−65.
(3) Ducker, W. A.; Senden, T. J.; Pashley, R. M. *Nature* **1991**, *353*, 239−41.
(4) Israelachvili, J. *Intermolecular and Surface Forces,* 2nd ed.; Academic Press: London, 1991.
(5) Fraxedas, J.; Garcia-Manyes, S.; Gorostiza, P.; Sanz, F. *Proc.. Natl. Acad. Sci. U.S.A.* **2002**, *99*, 5228−32.
(6) Morant, C.; Garcia-Manyes, S.; Sanz, F.; Sanz, J. M.; Elizalde, E *Nanotechnology* **2005**, *16*, 211−7.
(7) Garcia-Manyes, S.; Guell, A. G.; Gorostiza, P.; Sanz, F. *J. Chem. Phys.* **2005**, *123*, 11471−6.
(8) Garcia-Manyes, S.; Oncins, G.; Sanz, F. *Biophys. J.* **2005**, *89*, 1812−26.
(9) O'Shea, S. J.; Welland, M. E. *Langmuir* **1998**, *14*, 4186−97.
(10) Rief, M.; Gautel, M.; Oesterhelt, F.; Fernandez, J. M.; Gaub, H. E. *Science* **1997**, *276*, 1109−12.
(11) Biggs, S.; Mulvaney, P. *J. Chem. Phys.* **1994**, *100*, 8501−5.
(12) Biggs, S.; Mulvaney, P.; Zukoski, C. F.; Grieser, F. *J. Am. Chem. Soc.* **1994**, *116*, 9150−7.
(13) Larson, I.; Drummond, C. J.; Chan, D. Y. C.; Grieser, F. *J. Am. Chem. Soc.* **1993**, *115*, 11885−90.
(14) Li, Y. Q.; Tao, N. J.; Pan, J.; Garcia, A. A.; Lindsay, S. M. *Langmuir* **1993**, *9*, 637−41.
(15) Hu, K.; Bard, A. J. *Langmuir* **1997**, *13*, 5418−25.
(16) Zhang, J. H.; Yoon, R. H.; Mao, M.; Ducker, W. A. *Langmuir* **2005**, *21*, 5831−41.
(17) Larson, I.; Drummond, C. J.; Chan, D. Y. C.; Grieser, F. *Langmuir* **1997**, *13*, 2109−12.
(18) Biggs, S.; Proud, A. D. *Langmuir* **1997**, *13*, 7202−10.
(19) Liu, J. F.; Min, G.; Ducker, W. A. *Langmuir* **2001**, *17*, 4895−903.
(20) Hu, K.; Bard, A. J. *Langmuir* **1997**, *13*, 5114−9.
(21) Hu, K.; Chai, Z.; Whitesell, J. K.; Bard, A. J. *Langmuir* **1999**, *15*, 3343−7.
(22) Frisbie, C. D.; Rozsnyai, L. F.; Noy, A.; Wrighton, M. S.; Lieber, C. M. *Science* **1994**, *265*, 2071−4.
(23) Janshoff, A.; Neitzert, M.; Oberdorfer, Y.; Fuchs, H. *Angew. Chem., Int. Ed.* **2000**, *39*, 3213−37.

10.1021/ac0510437 CCC: $33.50
Published on Web 11/22/2005

studied as a function of the chemical composition.[24] Hence, the so-called "chemical force microscopy" (CFM) operation method,[25] which has been used recently to study the interactions between proteins and ligands,[26,27] single-bond rupture forces,[28−35] active enzyme interactions,[36] chirality,[37] hydrophobic interactions,[25,38,39] and cell membrane interactions. When the surface, the tip, or both surface and tip are functionalized with a ionizable group the term "force titration" has been used.[40] The aim of this particular technique is to measure the forces that arise between the tip and the surface as a function of pH and thus to measure the pK_a of surface ionizable groups at the nanometer scale through the plotting of the adhesion force that arises between a chemically derivatized tip and the ionizable surface sample as a function of pH value. This method constitutes a parallel approximation to surface pK_a determination where the silicon sphere attached to the cantilever has been replaced with a COOH self-assembled monolayer (SAM) covalently bound to the cantilever surface, which presents its own acid−base equilibrium. As long as this SAM acid−base equilibrium is well known, the control of the tip ionization degree (and charge) allows us to measure directly the variations in charge of the target surface and therefore the determination of its surface pK_a. So far, most of the studies have involved both tip and surface being functionalized with the same ionizable group in order to determine the tip−surface pK_a group, and the shape of the adhesion force versus pH curve has been shown to strongly depend on the ionic strength of the measuring system.[41] Two recent papers have also dealt with titration force microscopy in which tip and sample are differently chemically modified.[42,43]

On the other hand, supported lipid bilayers (SPB, also known as BLM, black lipid membranes) have been subjects of great interest as model cell membranes, to study cell−cell recognition in the immune system, adhesion of cells, phospholipid diffusion, protein binding to lipid ligands, and membrane insertion of proteins.[44,45] AFM has also become a powerful tool[46] in the study of such SPBs. Both molecular structure and morphological aspects have been demonstrated[47−49] by imaging lipid bilayers in aqueous media. However, it is only by force measurements (through the force spectroscopy mode) that we can obtain valuable information regarding phospholipid interaction forces, such as those generated either by DLVO forces, by hydration forces, or by steric forces.[50] Recent contributions have dealt with membrane nanomechanics using force spectroscopy, especially regarding the measurement of the elastic/plastic behavior of the bilayer as a function of its composition or the interaction with chemically modified probes.[51] Indeed, protein binding to lipid bilayers is known to strongly depend on the pH. Surface charges also play a key role in regulating cell adhesion and aggregation phenomena, antigen−antibody or cell−drugs interactions. A wide variety of phospholipid molecules is present in natural membranes. In principle, surface charge is determined by the chemical composition of the hydrophilic head of the molecule. While phosphatidylcholine and phosphatidylethanolamine are zwitterionic and thus have a net zero charge at neutral pH, other headgroups such as phosphatidylglycerol exhibit a net negative charge. Most natural membranes display a globally negative charge because of the presence of variable quantities of negatively charged phospholipids. Amid all the different phospholipid molecules, one of the most widespread in nature is phosphatidylcholine. This head is composed of one ionizable group, namely, the oxygen bound to the phosphate group. This constitutes a complex and interesting substrate, and the determination of the surface pK_a is extremely interesting from a nanometric point of view. Conversely, an example of natural negatively charged bilayer is the lipidic membrane of *Escherichia coli*. Besides phosphatidylethanolamine, the *E. coli* membrane is composed of phosphatidylglycerol and cardiolipin, thus exhibiting global negative charge.

Many techniques are able to determine the presence of ionizable groups, such as microelectrophoresis, ion-exchange chromatography, surface potential measurements,[52] or classical chemical titrations.[53] However, in the particular case of titrating lipid bilayers, these techniques demand relatively high concentrations of liposomes and have to be conducted first in liposome form and second in solution. The results are then the average of the electrochemical properties of liposomes present in solution and not the intrinsic pK_a values of the bilayers formed on a substrate with those liposomes. In fact, there might be a difference in the behavior of ionizable groups present on the surfaces compared to their behavior in solution,[54] but a direct titration of the SPB has not been reported to date. To accurately measure surface charges and surface pK_a, a local probe technique such as AFM is

(24) Noy, A.; Sanders, C. H.; Vezenov, D. V.; Wong, S. S.; Lieber, C. M. *Langmuir* **1998**, *14*, 1508−11.
(25) Noy, A.; Frisbie, C. D.; Rozsnyai, L. F.; Wrighton, M. S.; Lieber, C. M. *J. Am. Chem. Soc.* **1995**, *117*, 7943−51.
(26) Florin, E. L.; Rief, M.; Lehmann, H.; Ludwig, M.; Dornmair, C.; Moy, V. T.; Gaub, H. E. *Biosens. Bioelectron.* **1995**, *10*, 895−901.
(27) Moy, V. T.; Florin, E. L.; Gaub, H. E. *Science* **1994**, *266*, 257−59.
(28) Beulen, M. W. J.; Bugler, J.; de Jong, M. R.; Lammerink, B.; Huskens, J.; Schonherr, H.; Vancso, G. J.; Boukamp, B. A.; Wieder, H.; Offenhauser, A.; Knoll, W.; van Veggel, F. C. J. M.; Reinhoudt, D. N. *Chemistry: Eur. J.* **2000**, *6*, 1176−83.
(29) Kado, S.; Kimura, K. *J. Am. Chem. Soc.* **2003**, *125*, 4560−4.
(30) Skulason, H.; Frisbie, C. D. *J. Am. Chem. Soc.* **2002**, *124*, 15125−33.
(31) Skulason, H.; Frisbie, C. D. *J. Am. Chem. Soc.* **2000**, *122*, 9750−60.
(32) Conti, M.; Falini, G.; Samori, B. *Angew. Chem., Int. Ed.* **2000**, *39*, 215.
(33) Bustanji, Y.; Samori, B. *Angew. Chem., Int. Ed.* **2002**, *41*, 1546−8.
(34) Wenzler, L. A.; Moyes, G. L.; Olson, L. G.; Harris, J. M.; Beebe, T. P. *Anal. Chem.* **1997**, *69*, 2855−61.
(35) Wenzler, L. A.; Moyes, G. L.; Raikar, G. N.; Hansen, R. L.; Harris, J. M.; Beebe, T. P.; Wood, L. L.; Saavedra, S. S. *Langmuir* **1997**, *13*, 3761−8.
(36) Fiorini, M.; McKendry, R.; Cooper, M. A.; Rayment, T.; Abell, C. *Biophys. J.* **2001**, *80*, 2471−6.
(37) McKendry, R.; Theoclitou, M. E.; Rayment, T.; Abell, C. *Nature* **1998**, *391*, 566−8.
(38) Dicke, C.; Hahner, G. *J. Phys. Chem. B* **2002**, *106*, 4450−6.
(39) Skulason, H.; Frisbie, C. D. *Langmuir* **2000**, *16*, 6294−7.
(40) Vezenov, D. V.; Noy, A.; Rozsnyai, L. F.; Lieber, C. M. *J. Am. Chem. Soc.* **1997**, *119*, 2006−15.
(41) Smith, D. A.; Wallwork, M. L.; Zhang, J.; Kirkham, J.; Robinson, C.; Marsh, A.; Wong, M. *J. Phys. Chem. B* **2000**, *104*, 8862−70.
(42) Wang, B.; Abdulali-Kanji, Z.; Dodwell, E.; Horton, J. H.; Oleschuk, R. D. *Electrophoresis* **2003**, *24*, 1442−50.
(43) Wang, B.; Oleschuk, R. D.; Horton, J. H. *Langmuir* **2005**, *21*, 1290−8.
(44) Sackmann, E. *Science* **1996**, *271*, 43−8.
(45) Mueller, H.; Butt, H. J.; Bamberg, E. *J. Phys. Chem. B* **2000**, *104*, 4552−9.
(46) Desmeules, P.; Grandbois, M.; Bondarenko, V. A.; Yamazaki, A.; Salesse, C. *Biophys. J.* **2002**, *82*, 3343−50.
(47) Kaasgaard, T.; Leidy, C.; Ipsen, J. H.; Mouritsen, O. G.; Jorgensen, K. *Single Mol.* **2001**, *2*, 105−8.
(48) Slade, A.; Luh, J.; Ho, S.; Yip, C. M. *J. Struct. Biol.* **2002**, *137*, 283−91.
(49) Schneider, J.; Dufrene, Y. F.; Barger, W. R., Jr.; Lee, G. U. *Biophys. J.* **2000**, *79*, 1107−18.
(50) Dufrene, Y. F.; Boland, T.; Schneider, J. W.; Barger, W. R.; Lee, G. U. *Faraday Discuss.* **1998**, 79−94.
(51) Schneider, J.; Barger, W.; Lee, G. U. *Langmuir* **2003**, *19*, 1899−907.
(52) Cevc, G. *Biochim. Biophys. Acta* **1990**, *1031*, 311−82.
(53) Tsui, F. C.; Ojcius, D. M.; Hubbell, W. L. *Biophys. J.* **1986**, *49*, 459−68.
(54) Dai, Z.; Ju, H. X. *Phys. Chem. Chem. Phys.* **2001**, *3*, 3769−73.

needed to investigate the actual surface charges of an ensemble of a few molecules. The determination of such intrinsic electrostatic properties at a local level is important not only from a biological point of view but also from an analytical point of view, since nanometric sensors are being developed and demand nanometric probes to investigate the physicochemical properties of the target surface.[55−58]

The aim of this work is twofold. First, to show that the electrostatic properties of the surface can be properly investigated with a carboxyl-terminated probe, even in complex systems such as lipid bilayers. The functionalized AFM tip acts thus as a nanotitration agent able to sense the changes of ionization degree that the surface undergoes. These measurements can be compared to acid−base titrations of classical analytical chemistry with a weak acid (in this case, the acid group being attached to the tip), performed at the nanoscale, in solution and directly onto a supported surface. We now aim to extend the works available in the literature that deal with a large number of surface chemistries toward studying the chemical properties of biologically relevant lipid bilayers, both synthetic and natural. Second, we aim to proof that both approach and retract curves can be used to measure the interaction forces between tip and bilayer. Although most studies concerning titration force microscopy have only dealt with the retracting curve of the force plot (adhesion force), their interpretation depends on electrostatic forces but also on hydrogen bonding and, in this case, is further complicated by the rupture of the lipid bilayer during the indentation approach−retract cycles. The approach portion of the curve (previous to contact) is thus expected to provide a better measurement of the interactions with the unmodified lipid bilayer. So far, only one work has dealt with both approach and retract curves, to measure the surface charges of microbial cells.[59] In this case, however, it is not possible to relate the experimental results with the changes in the degree of ionization of particular chemical groups in the surface, because the cell surface is composed of lipid bilayers, proteins, and glycans with different concentrations. In our study, we have taken advantage of the high sensitivity of the COOH-terminated probes to measure small surface charges (they are able to measure surface potencials as small as a few mV) and of a force spectroscopy system with high force resolution in order to quantify the ionization changes of a biologically relevant surface. This opens the possibility of studying local surface charges from a nanometric point of view and to determine the surface pK_a of ionizable groups present in the surface by combining complementary information obtained from both extending and retracting curves with a chemically COOH-terminated modified tip, which is of great interest for analytical chemistry.

MATERIALS AND METHODS

Sample Preparation and Recording Solutions. 1,2-Dimyristoyl-*sn*-glycero-3-phosphocholine (DMPC) and 1,2-dilauroyl-*sn*-glycero-3-Phosphocholine (DLPC) were purchased from Sigma (> 98%). *E. coli* polar lipid extract (nominally 67% phosphatidylethanolamine, 23.2% phosphatidylglycerol, and 9.8% cardiolipin) was purchased from Avanti Polar Lipids (Alabsater, AL). Basically, the polar lipid extract is the total lipid extract precipitated with acetone and then extracted with diethyl ether.[60] Liposomes of DMPC, DLPC, and *E. coli* polar lipid extract were obtained in the same way: lipids were dissolved in chloroform/ethanol (3:1) (Carlo Erba, analysis grade, at 99.9%) to give a final lipid concentration of 2 m*m*. This dissolution was kept at −10 °C. A 500-μL aliquot was poured in a glass vial, and the solvent was evaporated with a nitrogen flow, obtaining a lipid film at the bottom of the vial. The solution was kept in a vacuum overnight to ensure the absence of organic solvent traces. Then, water solution was added to a final lipid concentration of 500 μM. The vial was subjected to 30-s cycles of vortexing, temperature, and sonication until a homogeneous mixture was obtained. Temperature was set at 30 °C in the case of DLPC ($T_m = -2$ °C) and 45 °C in the case of DMPC ($T_m = 23$ °C) and *E. coli* extract ($T_m \sim 30$ °C), since DLPC is already in the liquidlike phase at room temperature whereas DMPC and *E. coli* extract need to be in the liquidlike phase to help the resuspension step in the liposome production process. The solution was finally sonicated for 20 min in order to have unilamellar liposomes and allowed to settle overnight at 4 °C always protected from light. Four aliquotes of 50 μL were poured in Eppendorf tubes, adding milli-Q water buffered with Hepes 10 mM/NaOH to a final pH 7.4). Prior to use, mica surfaces (Metafix, CLLS grade) were glued to Teflon disks with a water-insoluble mounting wax. A 50-μL aliquot of lipid solution was applied to cover ~0.5-cm^2 freshly cleaved mica sheet and allowed to deposit for 35 min. Finally, prior to the measurements, mica was rinsed three times with 100 μL of the aqueous measuring solution. Recording solutions of different pH were all set at constant ionic strength 0.01 m. Solutions in the pH range 3−6 were prepared with 0.01 *m* NaAc. For solutions in the pH range 6.5−8.5, 0.01 *m* HEPES solutions were used, and in the pH range 7.2−9.2 0.01 *m* TRIS solutions were used. Solutions in the pH range below 3 and above 9.5 were unbuffered and prepared with diluted 0.01 *m* HCl and NaOH, respectively.

Zeta Potential Measurements. ξ Potential measurements were performed with a Zetamaster Particle Electrophoresis Analyzer through which the velocity of the particles can be measured with a light-scattering technique by using the Doppler effect thanks to a pair of mutually coherent laser beams (5 mW, He−Ne laser at 633 nm). Zetamaster measures the autocorrelation function of the scattered light, and after the signal processing, it obtains the electrophoretic mobility and, finally, through the Henry equation, the ξ potential.

AFM Imaging. AFM images were acquired with a Multimode (Digital Instruments, Santa Barbara, CA) microscope controlled by a Nanoscope IV electronics (Digital Instruments, CA) in contact mode using V-shaped Si_3N_4 tips (OMCL TR400PSA, Olympus, Japan) cantilevers. The applied force was controlled by acquiring force plots before and after every image was captured so as to measure the distance from the set point value. The applied force was set to 1.5 nN, far below the yield threshold of the bilayer (6.12 ± 0.02 nN[8]) in the case of DLPC, which prevents plastic deformation of the bilayer during imaging acquisition.

(55) Ottenbacher, D.; Kindervater, R.; Gimmel, P.; Klee, B.; Jahnig, F.; Gopel, W. *Sens. Actuators, B: Chem.* **1992**, *6*, 192−6.
(56) Sugao, N.; Sugawara, M.; Minami, H.; Uto, M.; Umezawa, Y. *Anal. Chem.* **1993**, *65*, 363−9.
(57) Nikolelis, D. P.; Mitrokotsa, M. *Biosens. Bioelectron.* **2002**, *17*, 565−72.
(58) Nikolelis, D. P.; Petropoulou, S. S. E.; Theoharis, G. *Electrochim. Acta* **2002**, *47*, 3457−67.
(59) Ahimou, F.; Denis, F. A.; Touhami, A.; Dufrene, Y. F. *Langmuir* **2002**, *18*, 9937−41.
(60) Newman, M. J.; Wilson, T. H. *J. Biol. Chem.* **1980**, *255*, 10583−6.

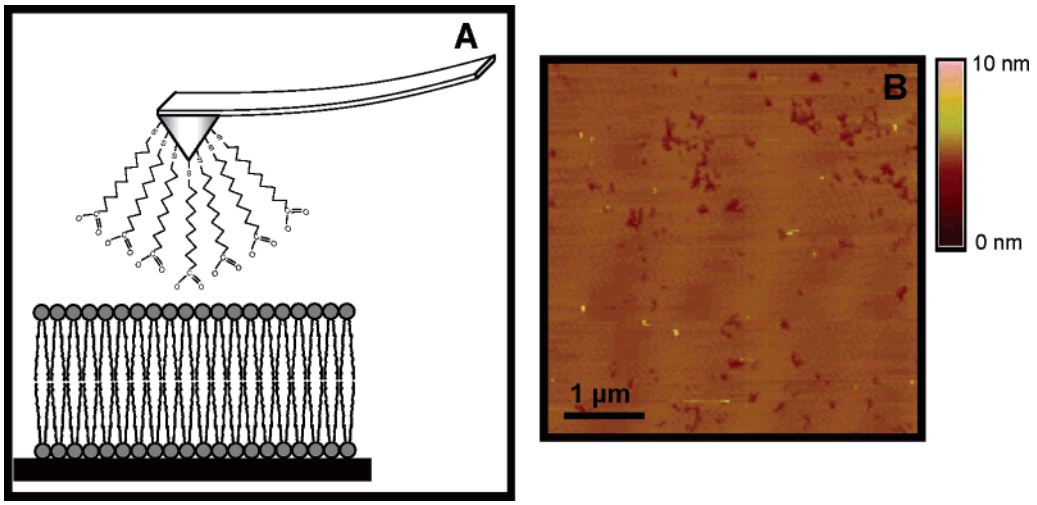

Figure 1. (A) Scheme of the thiol-functionalized tip approaching a supported lipid bilayer surface. (B) 5 × 5 μm^2 AFM contact mode image of a DLPC mica-supported bilayer. The applied force was set at 1.3 nN.

Force Spectroscopy. Force spectroscopy was performed with a Molecular Force Probe1-D (MFP), Asylum Research (Santa Barbara, CA). The MFP, based on AFM technology, has a one-dimensional, high-accuracy piezoelectric translator (10-μm range) located in the head that moves the tip toward (approach curve) and away from the sample (retract curve) in *z*-direction. A lineary variable differential transformer position sensor (<3-Å noise in 0.1−1-kHz bandwith) quantifies the real distance the *z*-piezo moves, therefore avoiding errors due to piezo hysteresis and other nonlinearities. Force plots were acquired using gold-coated V-shaped Si_3N_4 tips (OMCL TR400PB, Olympus) with a nominal spring constant of 0.09 N/m. Individual spring constants were calibrated using the equipartition theorem (thermal noise)[26] after determination of the tip sensitivity (V/nm) by measuring it at high voltages following several minutes of performing force plots to avoid hysteresis. Each full experiment was performed with the same cantilever, keeping the spot laser at the same position on the lever to avoid changes in the spring constant calculation.[61] Within the same experiment, the liquid was changed by slightly retracting the tip from the surface, carefully pipetting the buffer, and replacing it with a new solution with a different pH value. Then, a 5-min dwell time was used until force plots were acquired to equilibrate the system. The used liquid cell is a simple homemade Teflon cell designed according to the MFP 1D head design. The cell was cleaned with piranha solution before being used, thus giving rise to a complete hydrophobic surface that allowed the water solution droplet to totally cover the mica surface. Comparing results with different samples always gives rise to the same experimental trend, even though the absolute force values can greatly differ on account of the nature of the freshly formed self-assembled monolayer. The variability very much depends on the monolayer formed on the gold-coated tip surface. This typically gives rise to a variation in absolute force value of at most 30−35%. These error values agree with those reported in different papers concerning tip functionalization. In any case, the variability in the peak of the adhesion force does not vary significatively from tip to tip (~±0.2 pH unit). About 300 curves over more than five positions were obtained for each pH value. All force spectroscopy measurements were obtained at 20 ± 0.5 °C with *z*-piezo velocity $v = 0.6-1$ μm/s, *z*-piezo range 0.3−1 μm, and rate of data acquisition 10 000 points/s. Applied forces F are given by $F = k_c\Delta$, where Δ is the cantilever deflection. The surface deformation is given as penetration (δ) evaluated as $\delta = z - \Delta$, where z represents the piezoscanner displacement. In this paper, we focus on the data obtained both when tip is approaching and retracting from the surface, since both give rise to complementary information.

Chemical Modification of AFM Probes. Gold-coated cantilevers were placed into a 10-mm 16-mercaptohexadecanoic acid (Sigma)−2-propanol solution and kept at 4 °C overnight. Prior to use, tips were rinsed with 2-propanol and distilled water. Sonication was briefly applied to remove thiol aggregates that may be adsorbed. The quality of the SAMs was confirmed using contact angle measurements,[41] through which a gold surface was identically treated under the same experimental conditions as the used gold cantilevers.

RESULTS AND DISCUSSION

Highly Sensitive Detection of Surface Charge by COOH-Modified AFM Probes. Prior to studying the effects of pH on lipid charges, the ability of carboxyl-terminated probes to sense the electrostatic charges of surfaces was assessed by recording force curves using COOH-modified AFM probes (Figure 1A) on charged lipid bilayers deposited on mica (Figure 1B), in a solution at a fixed pH value. To play with lipid charge at constant pH, we took advantage of the fact that phosphatidylcholine (PC) lipid bilayers are known to bind cations thus increasing their electric surface charge, which has been demonstrated both experimentally[8,62,63] and through molecular dynamics simulations.[64,65] This increase in ionic strength gives rise to an increase of bilayer

(61) Proksch, R.; Schaffer, T. E.; Cleveland, J. P.; Callahan, R. C.; Viani, M. B. *Nanotechnology* **2004**, *15*, 1344−50.
(62) Eisenberg, M.; Gresalfi, T.; Riccio, T.; McLaughlin, S. *Biochemistry* **1979**, *18*, 5213−23.
(63) Makino, K.; Yamada, T.; Kimura, M.; Oka, T.; Ohshima, H.; Kondo, T. *Biophys. Chem.* **1991**, *41*, 175−83.
(64) Bockmann, R. A.; Hac, A.; Heimburg, T.; Grubmuller, H. *Biophys. J.* **2003**, *85*, 1647−55.
(65) Pandit, S. A.; Bostick, D.; Berkowitz, M. L. *Biophys. J.* **2003**, *84*, 3743−50.

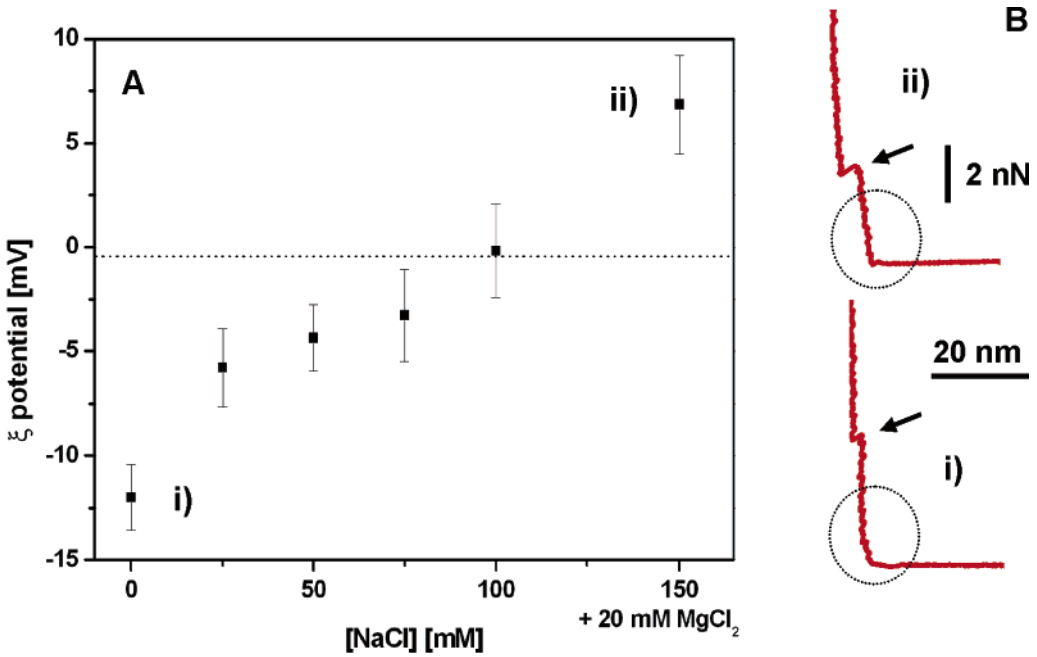

Figure 2. (A) ξ potential value vs ionic strength for a DMPC supported bilayer measured at pH 7.4. (B) Force−distance curves corresponding to the interaction of a −COO− chemically modified AFM probe at pH 7.4 with the DMPC bilayer under the ionic strength conditions corresponding to the points in (A); (i) 0 mM ionic strength; (ii) 230 mM ionic strength.

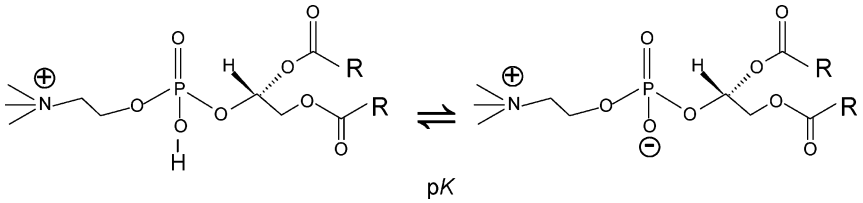

Figure 3. Chemical structure and acid−base equilibrium of a phosphatidylcholine headgroup.

compactness. For this particular experiment, we have used DMPC because it changes its global surface charge (from negative to positive) at moderate ionic strengths,[8,66] and we could measure it directly from the ζ potential of liposomes (Figure 2A).

PC heads are zwitterionic and thus globally uncharged at neutral pH, but they exhibit a negative ξ potential value in MilliQ water (pH 5.6). This has been interpreted in terms of hydration layers formed around the surface[67] and to the orientation of lipid headgroups.[63] As the ionic strength of the system is increased (while keeping a constant pH 7), liposomes acquire a less negative ξ potential until they reach a (slightly) positive surface charge. 16-Mercaptohexadecanoic acid has a pK_a in solution of ~4.7 ± 0.2. Thus, at pH 7, it is found in the COO^- form, i.e., negatively charged, and it is approximately neutral (but polar) below pH 4.

As shown in Figure 2A, in MilliQ water, DMPC liposomes exhibit a negative ξ potential value (−12.0 ± 1.6 mV), labeled as (i) in Figure 2A. In this case, surface and tip are both negatively charged, so an electrostatic repulsion should be expected when the tip is approaching the surface, as seen in the approaching force plot of Figure 2Bi). Conversely, as ionic strength is increased up to 0.23 *m*, a positive ξ potential value is measured (+6.38 ± 2.36 mV), indicated as (ii) in Figure 2A. In this case, then, attraction is expected between the positive sample and the negative tip. This is experimentally observed in the approaching force plot corresponding to the point ii in Figure 2B, where a small jump-to-contact (of ~90 pN) can be observed. It is thus clear that force spectroscopy with COOH-functionalized probes can be used to detect charged surfaces with ζ potentials as small as a few millivolts. Note that approach curves display a discontinuity in the contact region (pointed by arrows at ~4 nN) that corresponds to rupture of the ~4-nm thin lipid bilayer,[8] similar to that found in ionic[68] and covalent crystals.[7] The pH dependence of bilayer rupture will be discussed elsewhere (Sergi Garcia-Manyes et al., in preparation).

DLPC Titration. Phospholipid molecules are composed of a hydrophobic tail and a hydrophilic head. In the case of PC heads, only one ionized group is present, which is localized in the phosphate group. The chemical structure and the acid−base equilibrium are shown in Figure 3. Figure 4 shows the ξ potential versus pH plot for DLPC liposomes. The first region of the graph (1.5 < pH < 4.5) corresponds to the protonation/deprotonation of the oxygen atom from the phosphate group. The pK_a values for the ionizable group can be determined through the Henderson−Hasselbalch equation

$$\mathrm{pH} = \mathrm{p}K_a + \log \frac{f}{1-f}$$

where f is the degree of ionization of the surface to apply in the titration curve. From the electrokinetic measurements of Figure

(66) Garcia-Manyes, S.; Oncins, G.; Sanz, F. *Bioelectrochemistry*. Submitted.
(67) Egawa, H.; Furusawa, K. *Langmuir* **1999**, *15*, 1660−6.
(68) Arce, P. F. M. T.; Riera, G. A.; Gorostiza, P.; Sanz, F. *Appl. Phys. Lett.* **2000**, *77*, 839−41.

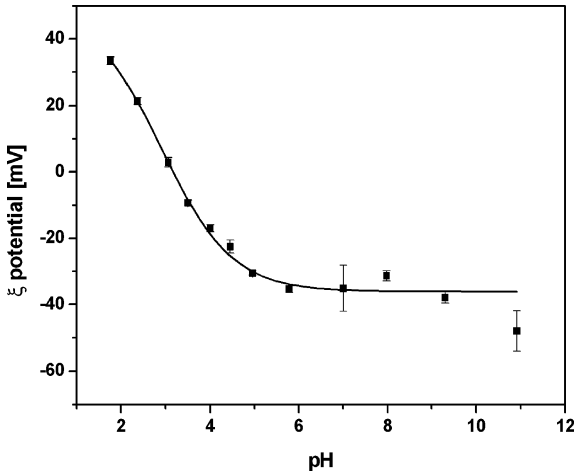

Figure 4. ξ potential value vs pH for unilamellar DLPC liposomes present in solution. Continuous black line stands for the best fit to the Boltzmann sigmoidal equation to the experimental data. Every point in the graph is the result of 10 independent measurements of the same solution, and bars stand for standard deviation within the measurements. In the case of pH 7, the error bar is the result of the independent measurement of the solution in three different days with the same equipment. (we used pH 7 as it is the more biologically relevant pH in order to check the reproductibility of the obtained data).

4 it is difficult to estimate the pK_a because the pH value does not reach a clear plateau at low pH values. The zero charge value is found at pH 3, where no net surface charge is measured. The continuous line is the best fit of the experimental data to a Boltzmann sigmoidal equation. The values obtained through electrokinetic measurements demand that liposomes are in solution, and the obtained values are a statistical mean of an ensemble of liposomes moving together under the effect of the electric field. To relate those results with those obtained on the surface, we have formed a DLPC supported lipid bilayer on a mica substrate. The coverage of the surface is nearly complete, as can be seen from the contact mode AFM image shown in Figure 1B. Here it is important to point out that titration force microscopy experiments were conducted on DLPC rather than on DMPC mostly because DMPC exhibits the main phase transition (solidlike → liquidlike) at $T_m = 23$ °C, which implies a high degree of topography reorganization,[69] which may alter the disposition of the bilayer on the surface. DLPC, in contrast, is liquid at room temperature and tends to homogeneously deposit onto mica surfaces, as has been shown in Figure 1B.

These electrokinetic measurements on free liposomes were then correlated to force spectroscopy measurements on supported bilayers. About 300 individual force plots on the DLPC surface were acquired with the COOH-terminated tip for every pH value (Figure 1A). During these titration experiments, the charge of the tip will also change as the pH is varied, due to the pK_a of the tip coating. This charge can be estimated from the pK_a value for a 16-mercaptohexadecanoic acid in solution, which has been calculated to be 4.78 ± 0.2.[70] Thus, far below this value, the molecule is protonated (COOH) and far above this point, the molecule adopts the $-COO^-$ form. Therefore, in solution around pH 4.78, half of the acid groups in the tip are protonated (COOH) and half deprotonated (COO^-), since the ionized fraction $f = 0.5$. However, we have to take into account that the pK_a value of the tip surface may vary within a limited range depending of every individual SAM and that it may be also shifted from the value reported in solution. The experimental approaching curves registered at different pH values are shown in Figure 5A. At 5 < pH < 11, a repulsion is observed, which slightly increases as the pH value increases. At pH 4.5−4.02, the net force is zero as seen

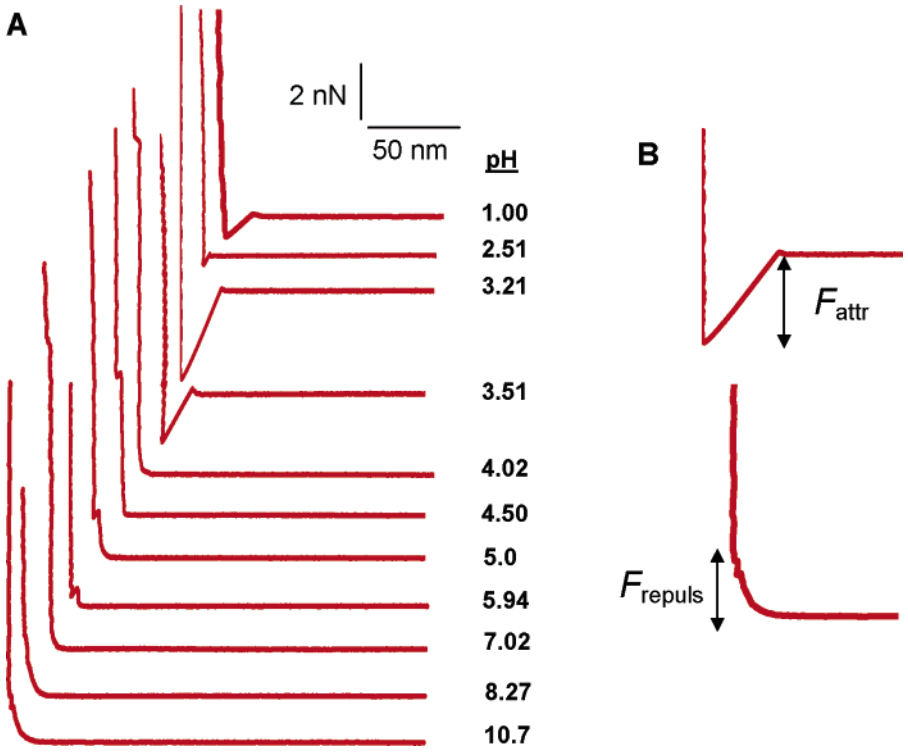

Figure 5. (A) Approaching force curves between a chemically COOH probe and a DLPC mica-supported lipid bilayer as a function of bulk pH. A repulsion between probe and surface is observed for 5 < pH < 11, no repulsion or attraction is observed for pH 4.02−4.50, and attraction between probe and surface is observed for 3.51 > pH > 1. (B) Scheme of the way of quantitatively measuring attractive and repulsive forces.

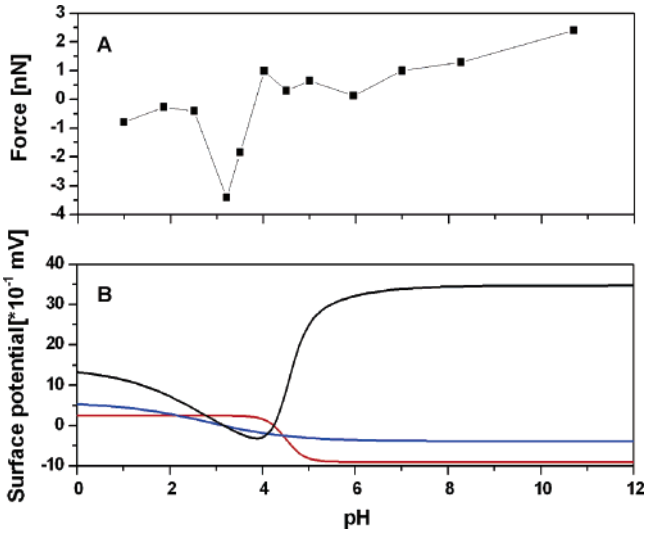

Figure 6. (A) Experimental interaction forces between a COOH chemically modified AFM probe and a supported DLPC membrane. Positive forces stand for repulsion and negative forces stand for attraction (jump to contact). (B) Qualitative representation of the surface charges of a COOH chemically modified probe and a DLPC supported lipid bilayer as a function of pH. Red line stands for tip charge evolution with pH. Blue line stands for surface charge evolution with pH. Black line stands for direct multiplication of blue and red lines. Note the high degree of accordance between black curve in (A) and curve (B).

from the absence of repulsion and jump to contact. This repulsion turns into an attraction at 2.8 < pH < 4.0. A huge jump to contact of ~2.3 nN is observed at pH 3.21. Below this pH value, a reduction in the jump to contact force is observed (pH 2.51, 120 pN). Finally, at pH 1, a higher snap-in of ~1.2 nN is observed. The interpretation of the shape of the approaching curves can be mainly done in terms of electrostatic interactions: at 5 < pH < 11, both surface and tip are negatively charged. Therefore, an electrostatic repulsion is expected, as experimental results confirm. Moreover, the higher the pH value, the more negatively charged the bilayer becomes (cf. Figure 4) and the repulsion becomes higher. The absence of repulsion or attraction between pH 4.5−4.0 can be interpreted if we take into account that within this small pH range lies the pK_a value for the COOH tip (pK_{tip}), and therefore, although the surface is negatively charged, the charge of the tip is sensibly reduced as the $-COO^-$ group binds protons. Further reducing the pH value results in a neutral (or very slightly) positively charged tip and a (still) negatively charged surface and thus the observed jump to contact for 3 < pH < 4.0 can be interpreted in terms of electrostatic attraction. At pH ~2.5−3, the lipid bilayer has virtually no charge (around the zero charge point) and therefore the jump to contact force should decrease if it is mainly related to electrostatic interactions. The important reduction in jump to contact (attractive) force experimentally observed (cf. Figure 5A) can be then also explained in terms of electrostatic interactions. Nonetheless, the increase in jump to contact attractive force for lower pH (pH ~1) cannot be explained in electrostatic terms, since both tip and surface are positively charged. The forces at every pH are outlined in Figure 6A. Positive forces stand for repulsion in the force plots (this repulsion being measured as the force at which the tip is in real contact with the hard wall surface taking as a reference the baseline; see F_{repuls} indication in Figure 5B), and negative forces stand for attraction between tip and surface (being measured as the jump to contact force; see F_{attr} in Figure 5B). Here it is worth pointing out that although extreme pH values are not physiologically relevant for most of the cases (even though some extremophile organisms can live in rather extreme pH values above pH 8.8 and below pH 5.5), we have experimentally proved that the studied lipid bilayers are able to withstand extreme pH values (i.e., 1 or 11) without losing their compactness and stability. This fact has been observed both through AFM imaging, where we observe homogeneous, continuous large membranes, and also through force spectroscopy, where we observe a discontinuity in the contact regime of the force plots at high loads, which is related to the membrane indentation that gives idea of membrane compactness.

As we have experimentally observed in Figure 2 and also in ref 8, chemical force microscopy in its titration force microscopy operation mode has the ability to detect small changes in surface potential through the force curves. To further understand the results shown in Figure 5, we have modeled the surface potential both for the tip and for the surface (Figure 6B), in an attempt to reproduce this behavior in terms of electrostatic interactions between 2 < pH < 11. Concerning the surface charge (blue line), we have fitted a Boltzmann sigmoidal curve (giving rise to results very similar to the shape obtained after applying Henderson equation) to the experimental data from Figure 4. Tip surface charge (red line), Q_1, has been simulated by applying the same Boltzman sigmoidal to mimic the acid−base equilibrium for the alkanethiol centered at pH 4.5. Surface potential (Q_2) value for a COO^--terminated SAM has been reported to be −140 mV,[40] and a very small positive charge (that could be present at very low pH values and also due to the hydration layers present around the phospholipid headgroup) is required in any case to fit our results. The black line is the result of the multiplication of both surface and tip charges to account for the pure electrostatic interactions arising as the tip approaches the surface, $F = kQ_1Q_2$. The shape of this line can be compared to the experimental interaction force obtained from the approaching curves (Figure 6A). Both qualitative surface−tip charge interaction plot and experimental force interaction match qualitatively well, indicating that electrostatic interaction may play the main role in phospholipid titration, especially in the pH range 2.5−11. Below this pH, the COOH (protonated) tip interacts with the surface where the phosphate group has been protonated. An H-bond interaction between tip and surface may account for this increase in the jump-to-contact force (Figure 5, pH 1 curve).[59]

Approaching curves have been studied in pioneering AFM work in order to elucidate electrostatic interactions between tip and surfaces.[71] Nonetheless, approaching curve analysis has deserved little attention in more recent CFM studies, which, instead, have mainly focused on the study of the adhesion force versus pH. Most of these studies have been performed by having the same functional group in both the tip and the surface.[40,41,72] The shape of the adhesion force graphs versus pH has been

(69) Garcia-Manyes, S.; Oncins, G.; Sanz, F. *Biophys. J.* In press.
(70) Calculated using Advanced Chemistry Development (ACD/Labs) Software Solaris V4.67 (1994−2005 ACD/Labs). 2005. Ref Type: Report.
(71) Butt, H. J. *Biophys. J.* **1991**, *60*, 777−85.
(72) Wallwork, M. L.; Smith, D. A.; Zhang, J.; Kirkham, J.; Robinson, C. *Langmuir* **2001**, *17*, 1126−31.

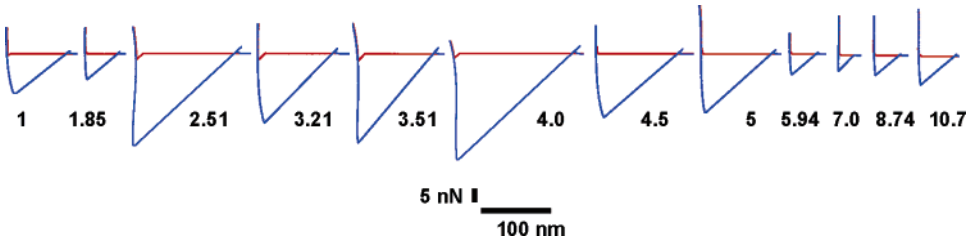

Figure 7. Evolution of the adhesion force represented as the force at which pull-off occurs (blue line in the force plot, detaching curve) as a function of pH between COOH chemically modified AFM probe and a DLPC supported bilayer.

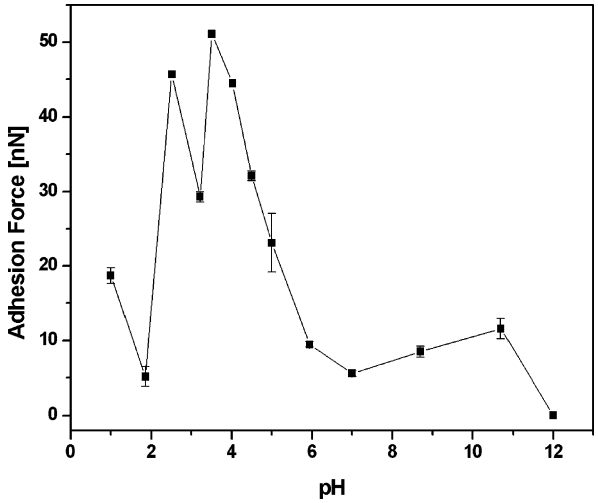

Figure 8. Evolution of the adhesion force between a COOH chemically modified AFM probe and a DLPC supported bilayer with pH.

proven to strongly depend on the ionic strength: While a sigmoidal shape similar to that observed in typical analytical titration curves is observed at high ionic strength for tip−COOH/HOOC$^-$ sample interaction,[40] a peak in the plot is observed at low ionic strengths, this peak being related to the "real" pK of the functional groups present on the surface.[41,73] The interpretation of such peaks has been made in terms of the high energy of the hydrogen bond formed between ionized and neutral acid groups coexisting on the surfaces near pK_a (∼28−30 kcal/mol),[74] much greater than the normal "weak" H−H hydrogen of a few kilocalories per mole. The formation of such an ionic hydrogen bond between the groups present on the tip and the groups present on the surface may be due to the solvent being expelled from the interaction volume when the tip and sample are brought into contact.[41] Therefore, adhesion measurements yielding peaks (low ionic strength) instead of a sigmoidal shape (high ionic strength) cannot be accounted for by a Johnson−Kendall−Roberts model treatment of adhesion. To corroborate our experimental results regarding the approaching curves, we have plotted the adhesion force versus bulk pH. Figure 7 shows a typical adhesion curve for every bulk pH value. Figure 8 shows the mean adhesion force for every pH (each point in the figure stands for the center (± standard deviation) of a Gaussian fitting of more than 300 individual curves taken at different positions of the surface). Interestingly, rather than observing a "typical" sigmoidal curve, the graph presents two main peaks centered at pH ∼2.5 and ∼4, of ∼45 and 50 nN, respectively. At pH <2, the surface is positively charged, since the phosphate group is fully protonated and the acidic group of the tip is in the COOH chemical form. A finite adhesion of ∼5−15 nN is found. This adhesion may be explained in terms of a "weak" hydrogen bond between tip and surface.[59] The pH range 2.5−3 corresponds to the isoelectric point of the surface. Consequently, about half of the phosphate groups of the phospholipid head are protonated and half deprotonated. Acidic groups of the tip are at this pH 100% (pK_{tip} ± 1) protonated. Therefore, a "ionic" hydrogen bond between tip and surface could account for this first adhesion peak. Increasing the pH value up to pH 3.21 results in a decrease in the adhesion force (∼29 nN). At this pH value, acidic groups of tip are protonated, whereas the surface is negatively charged, with the phosphate group fully deprotonated (cf. Figure 3). Therefore, at this particular pH, the contribution of aionic hydrogen bond is lower. At pH 3.5−4.0, the second peak is found. At this pH, the surface is negatively charged (phosphate group fully deprotonated) and the tip is about 50% protonated and 50% deprotonated (pH value near pK_{tip}, as related to the results observed upon the approaching curves). Therefore, here again a ionic hydrogen bond can be the responsible for this second adhesion peak. From this pH value on, the adhesion force decreases dramatically to a constant value of ∼3−5 nN. This decrease in the adhesion can be explained in terms of electrostatic repulsion between negatively charged tip and negatively charged surface, in the same way as repulsion is observed upon approaching curves in Figure 5 for pH >4.5.

Overall, both peaks are very clear and are perfectly consistent with the results obtained upon the approaching force curves. Moreover, all the peaks relate to the acid−base equilibria of the surface and seem to be a clear fingerprint of the protonation constants for both tip and surface.

***E. coli* Lipidic Membrane Titration.** Natural membranes possess a certain amount of negatively charged phospholipids, often mixed with PC and PE. Those negatively charged phospholipids, unlike phosphatidylcholine or phosphatidylethanolamine, possess a neutral group, and therefore, the phospholipid exhibits a net negative charge (located at the oxygen atom of the phosphate group) within a wide range of pH. In the case of the extract of *E. coli* membrane, a certain amount of phosphatidylglycerol ($CH_2CH(OH)CH_2OH$) and cardiolipin (diphosphatidylglycerol) is present mixed with PE. The increase of negative charge within the whole pH range is observed in Figure 9, where the ξ potential versus pH is shown. Unlike DLPC, in this case liposomes exhibit a net negative charge at all pH values, except pH ∼1, for which the surface exhibits a positive charge of ∼+5 mV.

(73) Smith, D. A.; Connell, S. D.; Robinson, C.; Kirkham, J. *Anal. Chim. Acta* **2003**, *479*, 39−57.
(74) Mautner, M. M. N.; Elmore, D. E.; Scheiner, S. *J. Am. Chem. Soc.* **1999**, *121*, 7625−35.

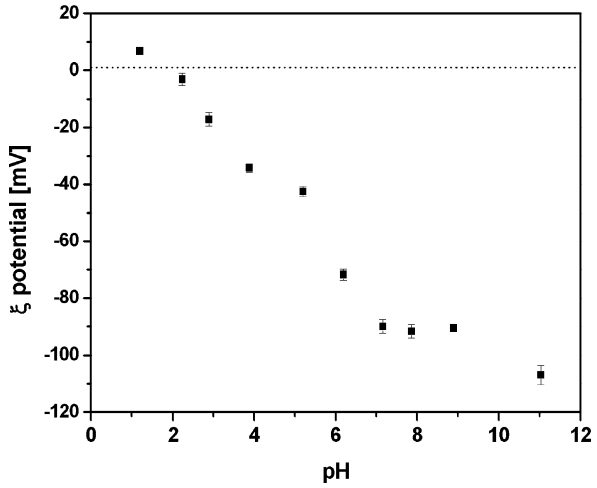

Figure 9. ξ potential value vs pH for unilamellar *E. coli* lipidic extract liposomes present in solution.

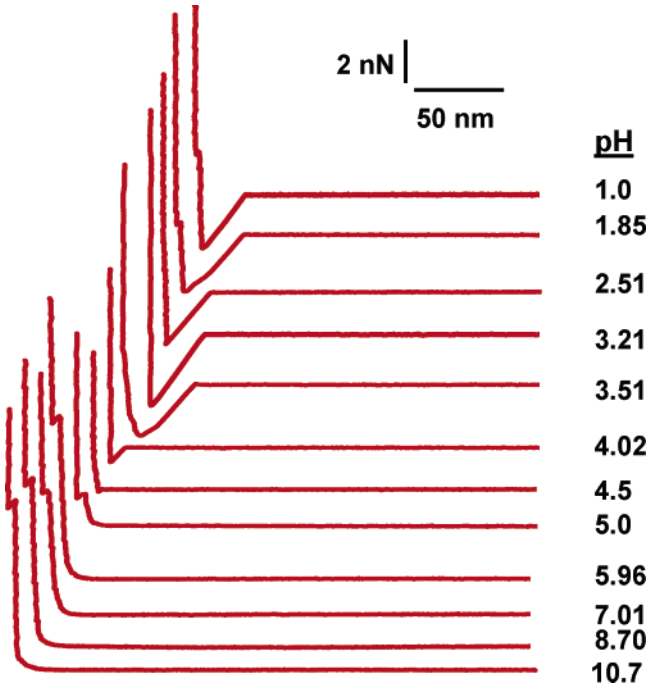

Figure 10. Approaching force curves between a chemically COOH probe and a *E. coli* mica-supported lipid bilayer as a function of bulk pH. A repulsion between probe and surface is observed for 5 < pH < 11, no repulsion or attraction is observed for pH 4.50, and attraction between probe and surface is observed for 4> pH > 1.

Assuming, as for the DLPC case described above, that approach force curves can be used to measure the electrostatic nature of the interactions arisen between the chemically modified tip and the phospholipid bilayer, we may expect an electrostatic repulsion at pH > pK_{tip}; at pH ~ pK_{tip} (pH ~4−4.5), we should expect neither an electrostatic repulsion nor an electrostatic attraction or snap-in; finally, at pH < pK_{tip} (protonated tip−negative surface), we should expect a strong snap-in. For pH <1 (out of our experimental conditions), a snap-in due to the H−H bond may be predicted. Figure 10 shows the evolution of approaching force curves with pH. Note that the jump-to-contact force is greater in this case (~3.3 nN) than in the case of DLPC, accounting for the increase in negative charge for 1 < pH < 4.5. At pH 4.5, the jump to contact is almost negligible, and for more basic pH values 5 <

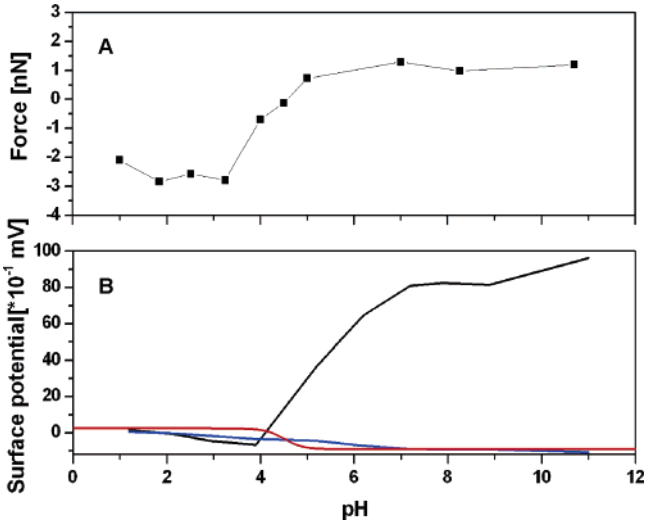

Figure 11. (A) Experimental interaction forces between a COOH chemically modified AFM probe and a supported DLPC membrane. Positive forces stand for repulsion, and negative forces stand for attraction (jump to contact). (B) Qualitative representation of the surface charges of a COOH chemically modified probe and a *E. coli* extract supported lipid bilayer as a function of pH. Red line stands for tip charge evolution with pH. Blue line stands for surface charge evolution with pH. Black line stands for direct multiplication of blue and red lines. Note the high degree of accordance between black curve in (A) and curve (B).

pH <11, a repulsion between probe and surface is also observed. Figure 11B shows a fit for the *E. coli* membrane similar to that shown in Figure 6B. The surface charge for tip simulation is the same as the one used in Figure 6B. Surface charges are obtained from experimental electrokinetic data shown in Figure 9. The multiplication of both tip and surface charges gives rise to the electrostatic interaction between surface and probe. The agreement between the qualitative approach for electrostatic interaction and the experimental interaction force (Figure 11A) is again quite high.

Concerning the retracting force plot, the evolution of the adhesion force versus pH is shown in Figure 12. In this case, only one acid−base equilibrium (the one corresponding to the tip, pK_{tip}) is reached. Only one peak, centered at pH ~3.8, is found in this case, exactly at the same pH at which we have found the first peak (~pK_{tip}) in Figure 8. Here again the same argumentation about high-energy hydrogen bond can account for the peak in the graph. However, in this case, no second peak is found, in agreement with the absence of acid−base equilibrium at the surface within this pH range, which is confirmed by ξ potential measurements.

CONCLUSIONS

In this work, we demonstrate that chemically modified probes are sensitive enough as to detect surface potentials as small as a few millivolts. Moreover, we show that chemically modified AFM tips can be used as a titration agent, provided that pK_{tip} and pK_{surf} show a ΔpK of ~1, and thus, it mimics a classical analytical chemistry titration where the titration agent is a "weak" acid. Approach force curves provide a simple measurement of the changes in surface charge. To interpret the experimental data, the forces between tip and sample can be estimated from their

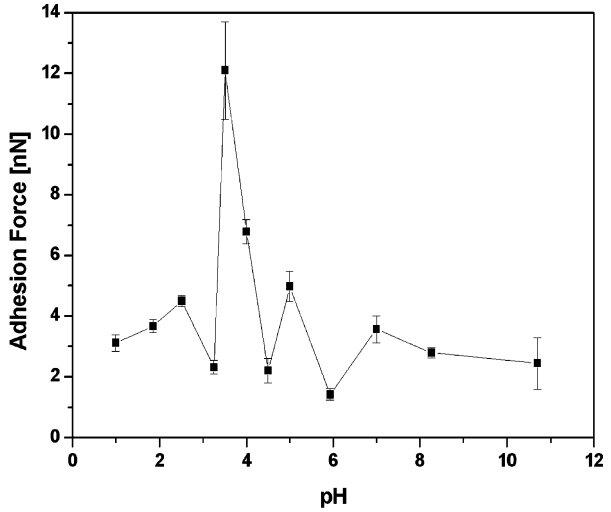

Figure 12. Evolution of the adhesion force between a COOH chemically modified AFM probe and a *E. coli* lipidic extract supported bilayer with pH.

respective surface charges, highlighting the electrostatic contribution of the interaction forces. Plots of adhesion force versus pH display a nonsigmoidal shape with a peak in the adhesion force that is related to the pK value, either of the tip or of the surface. This peak in the adhesion force may be attributed to high-energy ionic hydrogen bonds at low ionic strengths, as suggested by Smith and co-workers,[41] and therefore, the peak can be used as an experimental feature able to measure pK_a values of the studied surfaces at the nanometric scale, which are not accessible to electrokinetic experiments. This work shows the possibility of sensing surface charges present in a surface with nanometric resolution with a COOH chemically modified tip and to relate them to the underlying chemical equilibria taking place in the measuring system, which may be also of extreme importance in nanosensor applications.

ACKNOWLEDGMENT

S.G-M. thanks DURSI (Generalitat de Catalunya) for a grant and all for financial support through projects 2000SGR017 and AGP99-10. We thank Prof. Elisabeth Bosch (Department of Analytical Chemistry, University of Barcelona) for fruitful and helpful discussions, Dr. S. Vinzelberg (Asylum Research) for software development, Dr. T. Missana, CIEMAT (Madrid) for kindly allowing us to use the Zetamaster equipment, Òscar Domènech for supplying phospholipid, and Dr. François Bessueille for advise in probe functionalization.

Received for review June 13, 2005. Accepted October 24, 2005.

AC0510437